Semiconductor Science
and Technology

INVITED REVIEW

Atomic layer deposition of ZnO: a review

To cite this article: Tommi Tynell and Maarit Karppinen 2014 *Semicond. Sci. Technol.* **29** 043001

IOP Publishing Semiconductor Science and Technology
Semicond. Sci. Technol. **29** (2014) 043001 (15pp) doi:10.1088/0268-1242/29/4/043001

Invited Review

Atomic layer deposition of ZnO: a review

Tommi Tynell and Maarit Karppinen

Department of Chemistry, Aalto University, FI-00076 Aalto, Finland

E-mail: tommi.tynell@aalto.fi and maarit.karppinen@aalto.fi

Received 23 August 2013, revised 9 November 2013
Accepted for publication 9 January 2014
Published 26 February 2014

Abstract

Due to the unique set of properties possessed by ZnO, thin films of ZnO have received more and more interest in the last 20 years as a potential material for applications such as thin-film transistors, light-emitting diodes and gas sensors. At the same time, the increasingly stringent requirements of the microelectronics industry, among other factors, have led to a dramatic increase in the use of atomic layer deposition (ALD) technique in various thin-film applications. During this time, the research on ALD-grown ZnO thin films has developed from relatively simple deposition studies to the fabrication of increasingly intricate nanostructures and an understanding of the factors affecting the fundamental properties of the films. In this review, we give an overview of the current state of ZnO ALD research including the applications that are being considered for ZnO thin films.

Keywords: ZnO, atomic layer deposition, thin film

(Some figures may appear in colour only in the online journal)

1. Introduction

Zinc oxide is a wide band-gap semiconductor with a variety of useful properties that have made it a target of increasing attention in numerous fields of research. The high transparency of ZnO to visible light combined with its tunable electrical conductivity enable its use in applications ranging from thin-film transistors (TFTs) to the buffer layers of solar cells. ZnO's direct band gap of 3.37 eV at room temperature also means that it can be used in optoelectronic applications in the near-UV spectral range, including light-emitting diodes (LEDs) and photodetectors. Due to its piezoelectric properties, ZnO is also used in applications such as micro-electromechanical systems and sensors for detecting chemicals or gases [1–3].

The compound ZnO crystallizes in the hexagonal wurtzite structure and displays an intrinsic n-type conductivity which was originally attributed to oxygen vacancies and Zn interstitials formed during the synthesis process, but has since been shown to be caused by other unintentional impurities incorporated into the material during synthesis [4–6]. Hydrogen is a strong candidate for the identity of the donor that causes the n-type character, but the exact nature of its incorporation into ZnO is still unclear. Partly because of the strong n-type character of undoped ZnO, it has proven difficult to induce p-type conductivity in the material through the introduction of acceptor impurities. There are several reports of p-type conductivity achieved in ZnO by doping it with, for instance P or N, but the reproducibility and durability of this p-type doping are still problematic. The lack of p-type ZnO materials is hindering the applicability of ZnO in p–n junctions, so the solution of the p-type doping problem is one of the major challenges of ZnO research.

The attractiveness of ZnO is increased by its simplicity and the ease by which it can be synthesized in thin-film form using a variety of techniques. The deposition of ZnO thin films has seen a lot of research using all the applicable thin-film deposition methods from sputtering [7] to metal-organic chemical vapour deposition (MOCVD), [8, 9] molecular beam epitaxy (MBE) [10] and pulsed laser deposition (PLD) [10–12]. All of these deposition techniques have been used extensively in the research and fabrication of ZnO devices. Atomic layer deposition (ALD) is a chemical thin-film deposition method based on self-limiting, saturated surface reactions that result in highly conformal films and afford a great deal of control over the growth of the film. Until recent years, ALD saw relatively little use in the research of ZnO compared to the other deposition techniques, but the need for ever decreasing dimensions and increasing control

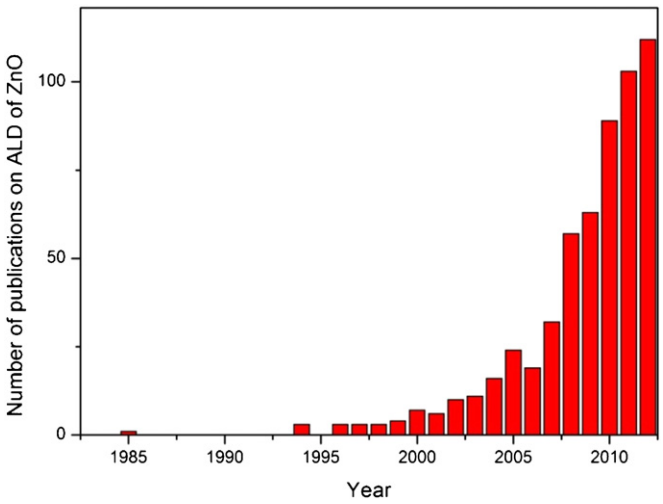

Figure 1. Number of ZnO ALD/ALE publications per year, retrieved using Scifinder.

in microelectronic applications has led to a remarkable rise in the interest in ALD in ZnO research. Figure 1 illustrates the development in the number of ZnO publications involving ALD or ALE (atomic layer epitaxy, an old name for ALD) in the last 30 years, clearly showing the rapidly increasing interest in the topic.

There are a number of exhaustive reviews published on ZnO itself, [2, 3] as well as its deposition in thin-film form employing the MOCVD, MBE and PLD techniques [7–12]. However, there are as of yet no comprehensive reviews on the use of ALD in the deposition of ZnO thin films, although there are reports that review its use for some specific applications or areas of research [13, 14]. As the importance of ALD in ZnO research is getting increasingly evident, we considered it useful to have a review collecting all the research that has been done on the ALD of ZnO. Therefore, it is the aim of this report to present the current state of research on ZnO ALD through the comprehensive overview of the existing publications on the topic.

2. Growth of ZnO thin films with ALD

2.1. Precursors and deposition parameters

The first precursors used for ALD growth of ZnO were zinc acetate (ZnAc) and water [15], where the reaction proceeds according to the following mechanism:

$$Zn(CH_3COO)_2^* + H_2O(g) \rightarrow ZnO^* + 2CH_3COOH(g) \quad (1)$$

where * denotes a surface species. ZnAc, however, requires a relatively high temperature to react with H_2O (the lowest reported deposition temperature using the ZnAc precursor is 280 °C), so other more reactive precursors have been developed for the ALD ZnO process since then. By far the most common Zn precursor used in ALD is diethyl zinc (DEZ) which reacts readily with H_2O through the following mechanism:

$$Zn(C_2H_5)_2^* + H_2O(g) \rightarrow ZnO^* + 2C_2H_6(g). \quad (2)$$

The reaction of DEZ with water is quite exothermic and can be used to deposit ZnO thin films at temperatures much lower than are needed for the ZnAc-based processes. Typical deposition temperatures for DEZ-based ZnO deposition processes are in the range of 100–200 °C, but the DEZ precursor has been successfully used even at room temperature and at temperatures as high as 600 °C.

Dimethyl zinc (DMZ), which bears a close resemblance to DEZ, is also sometimes used as the Zn precursor in ALD ZnO processes, and its reaction mechanism with H_2O is very similar to the DEZ-based process:

$$Zn(CH_3)_2^* + H_2O(g) \rightarrow ZnO^* + 2CH_4(g). \quad (3)$$

Despite seeing rather little use compared to DEZ, the DMZ precursor can be used in more or less the same range of deposition temperatures, although the temperature ranges for steady growth, the limits of the so-called ALD window, are generally reported to be slightly lower for DMZ. In a study investigating the effect of the Zn precursor choice on the properties of ZnO thin films, it was found that DMZ results in a slightly higher growth rate compared to DEZ, and the orientation of the resultant ZnO thin films is also different, but otherwise DMZ and DEZ produce ZnO films of equal quality [16].

Besides ZnAc, DMZ and DEZ, elemental Zn and $ZnCl_2$ have been used as Zn precursors in ZnO processes, but these require exceedingly high deposition temperatures and result in quite low deposition rates [17]. Methyl zinc isopropoxide, $(CH_3)Zn(OCH(CH_3)_2)$, is another potential Zn precursor that can be used at relatively low deposition temperatures and results in a relatively high growth rate, but it has not seen any use beyond the study that first reported it [18].

In addition to water, several other oxygen sources, including O_2, O_3 and N_2O, have been used in ZnO depositions with DEZ or DMZ. They can all be used to reach growth rates similar to the H_2O-based processes, but require higher deposition temperatures (significantly higher in the case of N_2O). Oxygen and water have also been used in a plasma form in plasma-enhanced ALD (PEALD) processes, which can be employed to grow films with a higher degree of stoichiometry at lower temperatures due to the higher reactivity of the plasma oxygen source. The various combinations of precursors along with the substrate materials and deposition temperatures employed are collected in table 1.

Table 1 clearly demonstrates the fact that DEZ is the preferred Zn precursor in ZnO ALD processes. While the other potential Zn precursors can also be used in the deposition of a variety of ZnO thin films, there are no particular disadvantages related to the use of DEZ, so it appears set to retain its position as the ALD Zn precursor of choice for the foreseeable future.

Looking at the deposition temperatures listed in table 1, it is apparent that ZnO can be deposited at almost any temperature that is available in ALD reactors, but the reported temperature ranges for the ALD window show a lot of inconsistencies. Some of this is explained by the different combinations of precursor chemicals; the use of DMZ or plasma processes results in generally lower ALD window temperatures, while precursors such as ZnAc or N_2O raise the required temperatures. However, judging by the fact

Table 1. ALD processes reported for the growth of ZnO thin films. The growth per cycle (GPC) values displayed in the table are from inside the ALD window; if no ALD window is reported, representative values from the entire tested temperature range are displayed instead.

Zn precursors	O precursors	Substrates	Deposition T (°C)	ALD window (°C)	GPC (Å/cycle)	References
$Zn(CH_3COO)_2$	H_2O	Soda glass	290–360	–	0.9–1.2	[15]
$Zn(CH_3COO)_2$	H_2O	Sapphire (0 0 0 1)	350	–	0.4–3.0	[19]
Zn, $ZnCl_2$, $Zn(CH_3COO)_2$	O_2, H_2O	Sapphire, Si, GaN/sapphire, soda glass	480–500, 300–360	–	–	[17]
$Zn(CH_3COO)_2$	H_2O	Sapphire, glass	280–400	–	0.8–4.0	[20]
$Zn(CH_3COO)_2$	H_2O	–	60–350	280–350, 80–150, 100–180	1.8	[21]
$Zn(CH_3)_2$, $Zn(C_2H_5)_2$						
$Zn(CH_3)_2$, $Zn(C_2H_5)_2$	H_2O	Soda glass	120–350	–	0.5–2.5	[22]
$Zn(C_2H_5)_2$	H_2O	Borosilicate	90–235	105–165	2.7	[23–25]
$Zn(C_2H_5)_2$	H_2O	PET, glass, sapphire, Si	100–210	–	1.4–1.9	[26]
$Zn(C_2H_5)_2$	H_2O	Au, glass	RT–220	130–180	2.2	[27]
$Zn(C_2H_5)_2$	H_2O	Si (1 0 0)	100–220	–	2.0	[28]
$Zn(C_2H_5)_2$	H_2O, O_2	Al_2O_3-coated Si	180	–	2.06	[29]
$Zn(C_2H_5)_2$	O_3	SiO_2/Si	230–300	230–250	1.9	[30]
$Zn(C_2H_5)_2$	O_2	Si	180, 270	–	–	[31]
$Zn(C_2H_5)_2$	O_2 plasma	Si (1 0 0)	75–150	100–150	2.2	[32]
$Zn(C_2H_5)_2$	H_2O	Sapphire (0 0 0 1)	100–250	130–180	2.7	[33]
$Zn(C_2H_5)_2$	H_2O	Glass, Si (1 0 0)	90–200	100–180	1.9	[34]
$Zn(C_2H_5)_2$	H_2O	Si (1 0 0)	70–350	70–200	1.9	[35]
$Zn(C_2H_5)_2$	N_2O	Sapphire (0 0 0 1)	600	–	–	[36]
$Zn(C_2H_5)_2$	H_2O	Glass	140	–	2.5–2.7	[37]
$Zn(C_2H_5)_2$	H_2O	Si (1 0 0)	60–300	125–150	1.9	[38]
$Zn(C_2H_5)_2$	O_2 plasma	ZnO-coated Si	150	–	–	[39]
$Zn(CH_3)_2$, $Zn(C_2H_5)_2$	H_2O	Glass	90–270	120–170, 130–170	1.4, 1.3	[40]
$Zn(CH_3)_2$, $Zn(C_2H_5)_2$	H_2O	Glass, Si, sapphire, GaAs	60–250	110–180	1.8–1.9	[41]
$Zn(CH_3)_2$	O_2 plasma	Si	25–120	85–120	2.9	[42]
$Zn(C_2H_5)_2$	N_2O	Sapphire (0 0 0 1)	250–340	290–310	2.6–2.7	[43, 44]
$Zn(C_2H_5)_2$	N_2O	Sapphire (11–20)	600	–	–	[45]
$Zn(C_2H_5)_2$	H_2O plasma	Si (1 0 0), quartz	100–300	150–200	2.0–2.2	[46]
$Zn(C_2H_5)_2$	H_2O	Glass, Si	120–240	120–150	1.8	[47]
$Zn(C_2H_5)_2$	H_2O	Glass, Si, GaN/Al_2O_3	100–300	100–200	–	[48]
$Zn(C_2H_5)_2$	H_2O	PVP/Si	80–140	–	2.0	[49]
$Zn(C_2H_5)_2$	H_2O	Borosilicate	100–250	–	1.2	[50]
$Zn(C_2H_5)_2$	H_2O	Si, SiO_2/Si	150–400	–	0.5–2.0	[51]
$Zn(C_2H_5)_2$	O_2 plasma	Glass, Si	100–300	200–250	2.8	[52]
$Zn(C_2H_5)_2$	H_2O	Si (1 0 0)	25–200	–	–	[53]
$Zn(C_2H_5)_2$	O_2 plasma, H_2O plasma	Si (1 0 0)	100	–	1.5–2	[54, 55]
$Zn(C_2H_5)_2$, $Zn(CH_3)_2$	H_2O	Glass, Si	100–200	120–170	2.1, 2.7	[16]
$Zn(C_2H_5)_2$	H_2O	GaAs	180	–	1.8	[56]
$Zn(C_2H_5)_2$	H_2O	Si (1 0 0)	RT–140	–	0.8–2.2	[57]
$Zn(C_2H_5)_2$	H_2O	Glass, Si, GaN	100–240, 250–300	–	–	[58]
$Zn(C_2H_5)_2$	O_2, H_2O	Si (1 1 1)	150–300	190–210, 200–225	4.8, 3.0	[59]
$Zn(C_2H_5)_2$	H_2O	Si (1 0 0)	80–240	100–160	2.3	[60]
$Zn(C_2H_5)_2$	H_2O	6H-SiC	180–300	–	–	[61]
$Zn(C_2H_5)_2$	H_2O	Si (0 0 1)	25–150	–	1.2–1.6	[62]
$Zn(C_2H_5)_2$	H_2O	SiO_2/Si, MgO	70–190	130–170	2.35	[63]
$Zn(C_2H_5)_2$	H_2O	Al_2O_3/Si	200	–	–	[64]
$Zn(C_2H_5)_2$	H_2O	Glass, Si	75–250	200–250	1.8	[65]
$Zn(C_2H_5)_2$	H_2O	Si	40–200	110–160	1.7, 2.5	[66]
$Zn(C_2H_5)_2$	H_2O + O_2 plasma	Glass, Si (1 0 0)	200	–	1.5	[67]
$Zn(C_2H_5)_2$	H_2O	Si (1 1 1)	150, 300	–	1.8–2.1	[68]
$Zn(C_2H_5)_2$	H_2O	Si, GaN, graphene sapphire	150–300	–	–	[69]
$Zn(C_2H_5)_2$	O_2 plasma	SiO_2/Si	150	–	–	[70]
$Zn(C_2H_5)_2$	H_2O plasma	SiO_2/Si	100–250	100–250	1.1	[71]
$Zn(C_2H_5)_2$	H_2O	Glass	50–200	–	0.7–1.9	[72]

that several, in some cases quite different, values have been reported for the ALD window when using exactly the same precursors, it seems apparent that reactor design also plays a large role in determining the ALD window range for ZnO processes. Considering all the factors that might affect the growth in a typical ALD process from the placement of the temperature sensors to the shape and size of the reactor and delivery of the precursors, to name a few, it is not surprising to see variations in the reported ALD window temperature range. The ALD window for a typical ZnO ALD process using DEZ and H_2O as precursors can nonetheless be estimated to be around 110–170 °C. The growth per cycle (GPC), i.e. the thickness of the layer deposited by a single ALD cycle consisting of pulses of the zinc and oxygen precursors separated by purging steps, for a DEZ/H_2O process within this window is around 1.8–2.0 Å/cycle, although here too there is a lot of variation in the reported GPC values due to the effects from the reactor design and other process parameters such as the pulsing and purging times. The interplanar distances in the hexagonal unit cell of ZnO range from 2.48 Å for the (1 0 1) planes to 2.60 Å and 2.82 Å for the (0 0 2) and (1 0 0) planes, respectively, [27] so the typical growth rates for ZnO within the ALD window are close to the ideal monolayer growth values. *In situ* quartz crystal microbalance (QCM) studies have also been used to examine the effect of precursor pulsing and purging times on the growth rate of ZnO in a DEZ/H_2O process, and no effect was seen from changing the purging time, while a slight increase in growth rate was observed with longer pulsing times [27]. This effect, however, is small compared to the influence of the deposition temperature.

2.2. Basic properties of ALD ZnO films

ALD-grown ZnO crystallizes in the hexagonal wurtzite structure, and a high degree of crystallinity is usually obtained in the as-deposited films even when using relatively low deposition temperatures. The structure of the films can be controlled somewhat through the deposition temperature, which has been observed to affect the preferred orientation of the grains in ZnO films. At deposition temperatures below 70 °C the ZnO films exhibit a strongly preferred orientation along the *c*-axis (the ⟨0 0 2⟩ direction) [57, 72]. Above 70 °C, the ⟨1 0 0⟩ direction starts to become more and more prominent until at around 160–200 °C the grains are predominantly oriented along the *a*-axis [27, 35, 38, 40, 72]. Raising the deposition temperature further above 220 °C causes the preferred orientation to switch again to the one dominated by the ⟨0 0 2⟩ direction [38]. Again, there is some variation in the reported deposition temperature-influenced orientation characteristics of ZnO films, so most likely the other deposition parameters also have some influence on the films' orientation. The choice of precursor chemicals can also affect the ZnO growth mode, e.g. it has been reported that adding an O_2 pulse step before the H_2O pulse in a typical DEZ/H_2O process can be used to switch the film orientation from the ⟨1 0 0⟩ direction to the ⟨0 0 2⟩ direction [29]. A similar effect has also been reported for lengthening the purging time in a ZnAc-based process, i.e. longer pulsing times result in a preferred ⟨0 0 2⟩ grain orientation [20]. Deposition temperature, however, is the single most influential parameter in most ZnO processes in determining the preferred orientation of the films.

Apart from the preferred orientation, the process parameters and precursors have little effect on the structural properties of the ZnO films. However, the deposition temperature does have an effect on the stoichiometry of the ZnO structure, which has a large effect on the electrical properties of the films. Because the intrinsic n-type conductivity of ZnO originates from the presence of defects and impurities in the ZnO crystal, its electrical properties can be controlled by adjusting the amount of these defects and impurities. In ALD processes this is most easily achieved by controlling the deposition temperature, since it directly influences the reactivity of the precursors on the film surface and thus can have an effect on the stoichiometry of the film. The influence of the deposition temperature on the electrical properties of ALD-grown ZnO is seen in the increase of the films' conductivity with increasing deposition temperature, although at very high temperatures the films' resistivity will start to increase again. The minimum values for ZnO film resistivity are typically achieved with deposition temperatures of 200–220 °C. In this temperature range, resistivity values as low as 10^{-3} Ω cm have been achieved.

The electrical properties of ZnO films can also be adjusted by using PEALD instead of thermal ALD. O_2 plasma, the typical oxidizer in plasma processes, is much more reactive than H_2O, so it can produce a more stoichiometric film as it oxidizes Zn more completely. This reduction in oxygen vacancies and interstitial Zn reduces the intrinsic n-type carrier concentration of ZnO, resulting in films with higher resistivity [32, 52, 67]. Apart from the stoichiometry and the resulting different electrical properties, though, the plasma process produces ZnO films with generally the same properties as thermal ALD. The growth rate can be significantly different between the two processes due to the GPC value in PEALD being sensitive to the plasma exposure time [67]. The crystallite size of ZnO deposited with PEALD is also reported to be significantly smaller than with thermal ALD, which could also play a role in increasing the resistivity of the films [67].

3. Cation doping of ALD ZnO thin films

In an effort to control the electrical properties of ZnO, ALD has been used to deposit ZnO films with a variety of different doping elements, the most common of which has been aluminum. Aluminum-doped ZnO, with resistivity values as low as 10^{-4} Ω cm, is a particularly promising candidate for replacing indium tin oxide as a transparent conductive oxide (TCO) material. In other cases, the motivation for doping is to increase the resistivity, as in the case of doping with sulfur, for use of ZnO in transparent TFTs. Some studies have also exploited doping as a means to induce p-type conductivity in ZnO, which has been shown to be achievable by using nitrogen or phosphorus doping along with post-deposition annealing. The dopants that have been used in connection with ALD-grown ZnO as well as the precursors, substrates, deposition

Table 2. Dopants and the associated precursors and process parameters reported for ALD of doped ZnO films as well as the minimum room-temperature resistivity values reported.

Dopants	Doping levels (%)	Precursors	Substrates	Deposition T (°C)	Min. ρ (Ωcm)	References
Al	0–4	$Zn(C_2H_5)_2$, $Al(CH_3)_3$, H_2O	Sapphire, (0 0 0 1)	180	–	[73]
Al	0–4	$Zn(C_2H_5)_2$, $Al(CH_3)_3$, H_2O	Si (1 0 0), borosilicate, sapphire (0 0 0 1)	140–220	7.7×10^{-4}	[74]
Al	0–4	$Zn(C_2H_5)_2$, $Al(CH_3)_3$, H_2O	SiO_2/Si, glass	200	1.7×10^{-3}	[75, 76]
Al	4.8	$Zn(C_2H_5)_2$, $Al(CH_3)_3$, H_2O	Si (1 0 0), SiO_2/Si	200	2.5×10^{-3}	[77]
Al	0.7–4.9	$Zn(C_2H_5)_2$, $Al(CH_3)_3$, H_2O	Si (1 0 0), soda glass	120–300	1×10^{-3}	[78]
Al	0–5	$Zn(CH_3)_2$, $Zn(C_2H_5)_2$, $Al(CH_3)_3$, H_2O	Soda glass	200–250	1×10^{-3}	[22]
Al	2–5	$Zn(C_2H_5)_2$, $Al(CH_3)_3$, O_3	Si (1 0 0), SiO_2/Si	250	3.8×10^{-4}	[79]
Al	0–6.67	$Zn(C_2H_5)_2$, $Al(CH_3)_3$, H_2O	Borosilicate	160	2×10^{-3}	[80]
Al	1.4–7.7	$Zn(C_2H_5)_2$, $Al(CH_3)_3$, H_2O	Polymer template, Si	110, 250	–	[81]
Al	0–7.8	$Zn(C_2H_5)_2$, $Al(CH_3)_3$, H_2O	Glass, Si	200	7.1×10^{-4}	[82, 83]
Al	2–8	$Zn(C_2H_5)_2$, $Al(CH_3)_3$, H_2O	Sapphire	180	9.4×10^{-3}	[84]
Al	2–8	$Zn(CH_3)_2$, $Al(CH_3)_3$, H_2O	Si (1 0 0), glass	150–325	6.9×10^{-3}	[85]
Al	0–9.1	$Zn(C_2H_5)_2$, $Al(CH_3)_3$, H_2O	Quartz	150	4.4×10^{-3}	[86]
Al	0–10	$Zn(C_2H_5)_2$, $Al(CH_3)_3$, H_2O	Soda glass	200	9.7×10^{-4}	[87]
Al	1.1–10	$Zn(C_2H_5)_2$, $Al(CH_3)_3$, H_2O	Si	60–250	4.2×10^{-3}	[88, 89]
Al	2–10	$Zn(C_2H_5)_2$, $Al(CH_3)_3$, H_2O	Quartz	150	2.4×10^{-3}	[90]
Al	2.5–16.7	$Zn(C_2H_5)_2$, $Al(CH_3)_3$, H_2O	Glass, sapphire (0 0 0 1)	200, 250	1.4×10^{-3}	[91]
Al	0–20	$Zn(C_2H_5)_2$, $Al(CH_3)_3$, H_2O	Soda glass, borosilicate	160–220	6×10^{-3}	[92, 93]
Al	1–80	$Zn(C_2H_5)_2$, $Al(CH_3)_3$, H_2O	Sapphire, glass	200	6.5×10^{-4}	[94]
Al	0–100	$Zn(C_2H_5)_2$, $Al(CH_3)_3$, H_2O	Si (1 0 0)	177	2×10^{-3}	[28, 95, 96]
Al	0–100	$Zn(C_2H_5)_2$, $Al(CH_3)_3$, H_2O	Si	125	8×10^{-4}	[97, 98]
B	–	$Zn(C_2H_5)_2$, B_2H_6, H_2O	Borosilicate	105–165	2×10^{-4}	[24, 99–101]
Ga	0–5	$Zn(C_2H_5)_2$, $Ga(CH_3)_3$, H_2O	PET	130–210	8×10^{-4}	[26]
Ga	0–14	$Zn(C_2H_5)_2$, $Ga(C_2H_5)_3$, H_2O	Soda glass	100–350	–	[102]
Ga	–	$Zn(C_2H_5)_2$, $Ga(C_2H_5)_3$, H_2O	Sapphire	300	8.0×10^{-4}	[103]
Ge	0–50	$Zn(C_2H_5)_2$, $Ge(OCH_3)_4$, H_2O	Glass	100–350	–	[104]
H	–	$Zn(C_2H_5)_2$, H_2O, H_2 plasma	Si (1 0 0), glass, SiO_2/Si	200	7.3×10^{-4}	[105]
Hf	0–39	$Zn(C_2H_5)_2$, H_2O, $[(CH_3)(C_2H_5)N]_4Hf$	Sapphire, borosilicate	200	6×10^{-4}	[106]
Mn	6–8	Zn, $ZnCl_2$, O_2, H_2O, $Mn(thd)_3$, $Mn(acac)_3$	Sapphire, Si, GaN/ sapphire, soda glass	480–500	–	[17]
N	–	$Zn(C_2H_5)_2$, NH_3, H_2O	Sapphire (0 0 0 1)	150	17.9	[107, 108]
N	–	$Zn(C_2H_5)_2$, NH_3, H_2O	Fused silica	100–300	2	[109]
N	–	$Zn(C_2H_5)_2$, H_2O, N^+ ions	Borosilicate	190	–	[110]
P	0–3	$Zn(C_2H_5)_2$, $P(OCH_3)_3$, O_3	Si (1 0 0), SiO_2/Si	250	3×10^{-3}	[111]
P	–	$Zn(C_2H_5)_2$, H_2O, P_2O_5	SiO_2	300	68.5	[112]
P	0–5	$Zn(C_2H_5)_2$, $(CH_3)_3PO_4$, H_2O	Soda glass	160–220	2.5×10^{-2}	[92]
S	5–20	$Zn(C_2H_5)_2$, H_2S, H_2O	Quartz, Si, glassy carbon	120	7×10^{-3}	[113]
S	20–80	$Zn(C_2H_5)_2$, H_2S, H_2O	Si (1 0 0), SiO_2	110	2	[114]
S	20–80	$Zn(CH_3)_2$, H_2S, H_2O	Si (1 0 0)	100–300	–	[115]
Si	1.3–6.7	$Zn(CH_3)_2$, $[(CH_3)_2N]_3SiH$, H_2O_2	Si (1 0 0), glass, sapphire	300	9.2×10^{-4}	[116]
Sn	25–67	$Zn(C_2H_5)_2$, H_2O, $Sn[N(CH_3)_2]_4$	Si	120	–	[117]
Ti	1.2–4.8	$Zn(C_2H_5)_2$, $Ti[OCH(CH_3)_2]_4$, H_2O	Si	250	–	[81]
Ti	4.8–50	$Zn(C_2H_5)_2$, $Ti[OCH(CH_3)_2]_4$, H_2O	Si, SiO_2/Si, quartz	200	8.9×10^{-4}	[118]
Zr	0–8	$Zn(C_2H_5)_2$, $Zr[N(CH_3)_2]_4$, H_2O	Sapphire	180	1.3×10^{-3}	[119]

temperatures and doping levels employed are listed in table 2.

The scale of the research effort that has been directed at Al-doped ZnO is evident from the number of publications on it listed in table 2. The objective for many of these studies, apart from studying the reaction mechanisms involved, has been the lowering of ZnO's resistivity as low as possible, and several studies report resistivity values in the 10^{-4} Ω cm range. The optimal Al doping amount for minimizing resistivity varies from study to study, but is generally reported to be in the 2%–5% range. At higher Al contents the resistivity increases again as the solubility limit of Al into ZnO is exceeded, which is thought to lead either to the formation of separate Al_2O_3 phases or the spinel phase $ZnAl_2O_4$ [86, 95]. It should be kept in mind that in many studies on ALD of Al-doped ZnO the actual aluminum content of the films has not been verified with elemental analysis techniques, so the reported doping levels typically represent the expected doping level calculated from the ratio of the deposited aluminum oxide and ZnO layers rather than the actual aluminum content. However, it has been shown through *in situ* QCM studies that trimethyl aluminum (TMA), the aluminum precursor used in all the Al-doped ZnO studies, undergoes an exchange reaction with the ZnO surface that results in etching of the underlying film, proposed to happen through the following mechanism [28]:

$$ZnOH^* + Al(CH_3)_3 \rightarrow Al(CH_3)OH^* + Zn(CH_3)_2. \quad (4)$$

Table 3. Precursors, substrates and process parameters reported for ALE of ZnO.

Zn precursors	O precursors	Substrates	Deposition T (°C)	ALD window (°C)	GPC (Å/cycle)	References
$ZnCl_2$	O_2	Sapphire (0 0 0 1)	400–600	450–550	2.57	[120]
$ZnCl_2$	O_2, H_2O	GaN/Al_2O_3	480–500	–	0.5	[121, 122]
$Zn(C_2H_5)_2$	H_2O	Sapphire (0 0 0 1)	130–600	–	–	[123]
$Zn(C_2H_5)_2$	H_2O	GaN/Al_2O_3, sapphire	250	–	–	[124]
$Zn(C_2H_5)_2$	H_2O	Sapphire, Si (1 0 0)	170, 400	–	–	[125–127]
$Zn(C_2H_5)_2$, NH_3	H_2O	Sapphire (0 0 0 1)	150	–	–	[128]
$Zn(C_2H_5)_2$	H_2O	Sapphire (0 0 0 1)	350–550	–	2.6	[129, 130]
$Zn(C_2H_5)_2$	H_2O	Sapphire (0 0 0 1)	200	–	–	[131]
$Zn(C_2H_5)_2$	H_2O	Sapphire (0 0 0 1)	25–200	80–160	~4	[132, 133]
$Zn(C_2H_5)_2$	H_2O	Sapphire (10–10)	200	–	2.5	[134]
$Zn(C_2H_5)_2$, $Zn(CH_3)_2$	H_2O	GaN/Al_2O_3	300	–	–	[135, 136]
$Zn(C_2H_5)_2$	H_2O	Sapphire (0 0 0 1)	180	–	1.8	[137]

The aluminum oxide layers have also been observed to hinder the growth of ZnO on them [28], and together these effects often cause the actual aluminum content to differ from the intended one when depositing Al-doped ZnO films. The observed hindrance to ZnO growth varies between different studies, as the reported number of DEZ/H_2O ALD cycles required after a TMA/H_2O cycle to recover the normal growth rate is 4–12 cycles [28, 95, 97].

Besides affecting the carrier concentration and electrical conductivity of ZnO, Al doping has been observed to affect the films in other ways that can be useful for various applications. Firstly, the incorporation of Al_2O_3 layers into ZnO significantly reduces the surface roughness of the film, and by varying the amount of Al_2O_3 layers it is possible to tune the ZnO films' roughness for e.g. gas sensor applications [28, 86]. Al doping can also affect the crystallographic orientation of the grains in the ZnO film, causing the preferred orientation of the films to shift to the ⟨1 0 0⟩ direction (the orientation is also affected by the deposition temperature) [86, 87]. Most importantly, though, Al doping has little effect on ZnO's transmittance of visible light, with transmittance values of over 80% reported, making it possible to use Al-doped ZnO in TCO applications [74, 83, 85–87].

In the nitrogen and phosphorus doping studies listed in table 2 the objective has been to induce p-type conductivity in ZnO, which would enable the fabrication of homodiodes based on ZnO. This has been notoriously difficult for ZnO due to the high level of carrier doping from intrinsic defects. Nonetheless, both nitrogen and phosphorus doping were successfully used to turn ZnO's conductivity into p-type [107–112], although in all cases a post-annealing procedure was necessary to remove the n-type carrier doping from defects and donor impurities in ZnO. In the case of N-doped ZnO films, the typically used dopant is NH_3, which is proposed to occupy an O site in the ZnO structure with NH [107, 108]. The post-annealing at 1000 °C is necessary to remove the bonded H, leaving behind a nitrogen ion which will act as an electron hole donor in the ZnO structure. However, this will also result in a rather large resistivity in the film due to the ionic nature of the dopants, which will generally result in a larger reduction of carrier mobility compared to neutral impurities. In another study N was incorporated into ZnO by irradiating the film with a nitrogen ion beam after the ALD deposition [110]. Although p-type conductivity was not observed in this study, the carrier concentration and mobility of the film were found to decrease significantly due to the N ion implantation. Phosphorus is an amphoteric dopant, and the doping of ZnO with P using either trimethyl phosphite or trimethyl phosphate was observed to initially lead to n-type carrier doping of the film [92, 111]. The conductivity can subsequently be changed to p-type by annealing the film at 650–850 °C, whereby the phosphorus is thought to occupy a zinc site and form defect clusters with two adjacent zinc vacancies [111]. The resistivity of the p-type ZnO films achieved with either N or P doping, however, generally remains high compared to n-type ZnO which limits their applicability. The longevity of the p-type doping has also been an issue in previous attempts to fabricate p-type ZnO, and although the p-type behavior of the P-doped ZnO films was observed to remain stable for three months [111], it is unclear whether the deterioration of the p-type character can be avoided in these films in the long term.

4. Epitaxial growth of ZnO thin films

The growth of epitaxial films of ZnO by atomic layer epitaxy (ALE) is also possible with the right choice of substrate material. However, efforts to grow epitaxial ZnO films have seen relatively little interest compared to the large amount of research that has been done on regular ALD of ZnO, probably because the many potential applications of ZnO thin films do not strictly require the films to be epitaxial. The reported ALE processes of ZnO and the relevant process parameters are summarized in table 3.

As can be seen from table 3, the epitaxial growth of ZnO is typically achieved using sapphire substrates. Apart from the choice of substrate the process parameters, including the precursor chemicals, appear similar to those used in other ZnO ALD processes. The typically used *c*-plane sapphire is a structurally fairly good fit for ZnO and can be used to grow *c*-axis oriented monocrystalline ZnO films. Despite the 18% lattice mismatch between sapphire and ZnO, no buffer layer is necessary to obtain epitaxial ZnO films. GaN is another commonly used substrate in ZnO ALE, and it has a much lower lattice mismatch with ZnO compared to sapphire substrates which could be used to obtain higher quality ZnO films.

Besides choosing a suitable substrate to 'guide' ZnO to grow in an epitaxial manner, some studies report other ways to influence the crystal growth, such as using an electric field [123] or setting up an interrupted flow configuration in the reactor, both of which were found to improve the crystalline quality of the epitaxial ZnO films [132–134]. Generally, the deposition of epitaxial ZnO films with ALD is relatively simple with the right substrate; e.g. there are a wide variety of possible deposition temperatures listed in table 3, but the electrical properties of the epitaxial ZnO films are reported to be quite sensitive to changes in process parameters, with a study reporting a change in purging times causing the doubling of the carrier concentration of the ZnO film [135]. Similarly, using DMZ instead of DEZ as the zinc precursor was observed to cause a significant decrease in carrier concentration [136]. The reason for the apparent sensitivity to process conditions of epitaxial ZnO growth is not clear as no explanation is provided in the respective studies.

One of the more promising applications for epitaxial ZnO films is in the fields of optics and optoelectronics. Using ALE to deposit epitaxial ZnO films can be particularly valuable for so-called multilayer interference mirrors that are used in x-ray optics. This is due to the need for layered structures with highly precise layer thicknesses that can be fabricated relatively easily with ALE, and the deposition of such a structure has been successfully demonstrated [130]. The high quality of the ZnO films obtainable by ALE also makes the technique suitable for stimulated emission applications, where the epitaxial ZnO films can be used in photonic devices in the UV range [137].

5. Nanostructuring of ZnO with ALD

ALD is the ideal technique for the fabrication of nanostructured thin films due to the self-limiting nature of the surface reactions and the excellent conformality of the films [138]. Consequently, there is a wide variety of different nanostructures of ZnO that have been fabricated by using ALD. The applications of ZnO ALD in nanostructuring cover the whole field from coating various porous templates to fabricating nanotubes, nanorods and nanodots. This chapter will give an overview of the different types of nanostructures that ZnO ALD has been used to date.

5.1. ALD of ZnO nanorods and nanodots

The fabrication of nanostructures with one-dimensional (1D) or even zero-dimensional characteristics, i.e. nanorods or nanodots can have a huge influence on a material's performance in a variety of applications from gas sensing to electrical and optical applications, and as such there is a great interest in developing techniques for the accurate synthesis of such structures. ZnO nanorods or nanowires can be fabricated with ALD by taking advantage of lithography techniques [139–141] or by using a nanostructured template to deposit the nanorods on an underlying substrate [142–144]. ZnO nanowires can be realized with relatively simple spacer lithography [140, 141], although one study utilized a combination of phase-shift lithography and plasma etching that made it possible to fabricate a pattern of photoresist nanodots on a Si substrate that was used to etch out Si nanowires. Another coating of photoresist and the etching out of the Si nanowires could then be used to make a mask for the ALD of ZnO nanowires [139]. Similar phase-shift lithography processes have also been reported for the fabrication of 1D nanochannels or nanolines of ZnO, which were then used as templates for the synthesis of various 1D nanostructures or to fabricate a force sensor, respectively [145, 146]. The template-based studies on ALD ZnO nanorods make use of an anodic aluminum oxide (AAO) template, which is an Al_2O_3 substrate with vertically aligned nanopores with an aspect-ratio as high as 10^3 that can be easily controlled to adjust the diameter, depth or distribution of its pores. The use of such templates makes the fabrication of ZnO nanorods with ALD quite simple; the studies utilizing AAO all report the formation of high-quality ZnO nanorods. Moreover, although two of the studies do not comment on the length of the needed precursor exposure times, one study reports a pulsing time of 1 s for DEZ and H_2O, suggesting that prohibitively long pulsing times are not needed to achieve high-quality nanorods using AAO templates [142–144]. However, the aspect-ratio of the AAO template used in the study was reported as only 10:2, so much longer pulsing times will doubtless be needed when using AAO templates with aspect ratios in the upper part of the range [142].

ZnO ALD has also been utilized with films of nanoparticles that have nanoscale voids between them, allowing the diffusion of precursors through the structure and subsequent deposition of ZnO within the voids in the films [147, 148]. This can be used either to fabricate ZnO nanodots within the nanoparticle films [147] or to fill the voids with ZnO in order to affect the properties of the film [148]. The former was shown to result in a significant blue shift in the photoluminescence properties of ZnO [147], while the latter approach affected the mechanical as well as the photoluminescence and photosensitivity properties of the nanoparticle films [148].

There are a number of reports on the successful ALD fabrication of ZnO nanorods or nanodots even without the use of templates, although the scope of the described methods is somewhat limited and thus the approach has not attracted as much interest as methods utilizing masks or templates. These methods rely either on the use of very rough substrate surfaces [149] or on setting the process parameters in such a way that the film formation reactions cannot advance past the island-forming stage [150–152]. The ZnO islands fabricated in this manner can then be used as seeds for the growth of nanopillars [151], but overall the use of templates has proven more convenient for the nanostructuring of ZnO. There are also studies where ALD has been used to deposit a thin layer of ZnO, over which arrays of ZnO nanorods were subsequently fabricated by using a hydrothermal process [153–158]. Here the advantage of using ALD is mainly the ability to deposit textured high-quality films of ZnO to either act as a seed layer for the nanorod growth or to protect the substrate from the reagents of the hydrothermal process.

5.2. Templates for nanostructuring

In addition to their use as masks for the fabrication of nanorods and nanowires, nanoscale templates can be used as the substrates upon which ZnO is coated. This is often done with the intention of burning or otherwise disposing of the template after deposition in order to obtain ZnO nanotubes or other such nanostructures. The use of templates in this manner is very well suited for ALD processes due to the fact that ALD can be used to coat even very complex or high-aspect-ratio substrates in a conformal way. The templates used in ZnO nanostructuring via ALD can be roughly divided into two groups: Al_2O_3 templates and polymer templates. Almost all the reports on template-based ALD of ZnO use one of these templates, the only exception being bio-templates, which have been used in a few studies.

Besides the use of AAO templates in the fabrication of ZnO nanorods, the templates have been used to study the conformality of the ZnO coating inside the nanopores [159] and to make multi-segmented nanotubes that consist of a number of different materials forming parts of a single nanotube [160]. The ZnO deposition inside the pores of the AAO was found to be limited by diffusion, and the aspect ratio of the pores was observed to greatly affect the exposure time required for conformal coating, with a 120 s exposure time necessary for coating pores with an aspect ratio of ~5000. In addition to AAO, the coating of nanoporous alumina monoliths with an aspect ratio higher than 10^5 has been reported [161]. Despite the very large aspect ratio of the template, it was possible to achieve complete coverage, although exceedingly long exposure times of 70 min were required.

The polymer templates employed in ZnO nanostructuring exhibit a wide variety of polymer types as well as uses, which range from nanofiber templates [162–166] for nanotube fabrication to the use of lithography-modified polymer layers for the growth of ZnO nanoarrays [167]. Other uses for the ZnO coating of polymer templates include the protection of nylon fibers [168] and as a support for ZnO nanocrystal growth [169]. No longer than normal reactant pulsing times were reported to be necessary with the polymer templates, although significantly longer purging times, as long as 60 s, were needed to ensure that the reactants reached all the surfaces and to remove excess reactants.

The possibility to grow ZnO at relatively low temperatures has enabled the use of bio-templates in ZnO nanostructuring. One such approach has been to use cicada wings as templates, taking advantage of the fact that nanopillars on the wing surface block ZnO growth [170, 171]. In another study, the fibers of an eggshell membrane were coated [172], while another one used nanocellulose fibers to fabricate ZnO nanotubes [173]. Overall, the use of bio-templates in ZnO nanostructuring remains relatively unexplored and the field certainly possesses a lot of potential for novel applications. A SEM image of a cicada wing bio-template with ZnO deposited between the nanopillars on the wing surface is displayed in figure 2.

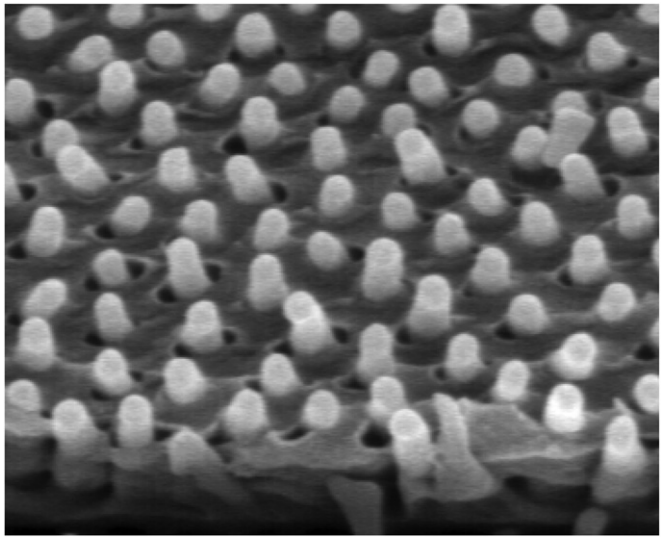

Figure 2. A SEM image of ZnO deposited on a cicada wing. Reprinted with permission from [170]. 2008 American Chemical Society©.

5.3. Core–shell nanostructures

Core–shell nanostructures are formed when a nanoscale structure, typically a particle or nanorod, is coated with a thin layer of another material. This can have several beneficial effects, from altering the properties of the core material to providing a carrier for the shell material, and it is no surprise that core–shell structures are the area of nanostructuring that has seen the most interest within ALD of ZnO.

The ZnO ALD process has been used to coat particles of Si [174], SiO_2 [175–178], TiO_2 [179], Al_2O_3 [180], polystyrene [181] and a number of other materials, mostly oxides [182–184]. The most common application for the ZnO core–shell particles is in catalysis, but ZnO on TiO_2, for example, can also be used in blocking UV radiation. A viscous flow reactor is sufficient for the particle coatings, provided that some sort of grid or fixture is implemented to keep the particles contained [175, 180, 182], though a fluidized bed reactor configuration has been used in several studies [176–179].

The coating of nanowires, nanotubes or nanorods with ZnO (or coating ZnO nanowires) can offer more possibilities for applications than particles, so there has been considerable research effort to study the use of ZnO in core–shell nanowire systems. Some of the more commonly studied structures include ZnO combined with Si or SiO_2 [185–194], SnO_2 [195–199], Al_2O_3 [200–202] and carbon nanotubes [203–205], but combinations of ZnO with several other materials have also been reported [206–216]. The motivation for these studies has been very application-centered, and the majority of them concentrate on either the photoluminescence or chemiresistive properties of the material system, which have applications in the optoelectronics and gas sensing fields, respectively. Typically, the nanowire part of the core–shell structures is prepared using another technique; surely due to the relative difficulty of fabricating nanowires with ALD. The shell part of the structure is then deposited using ALD, taking advantage of the strengths of the technique. For many of the studied ZnO

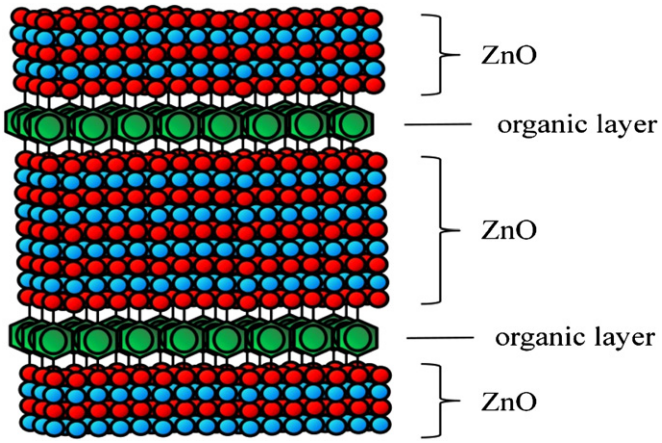

Figure 3. An illustration describing a part of a hybrid superlattice structure. Reprinted from [223], 2013 Elsevier BV©, with permission from Elsevier.

depositions on nanowires the necessary pulsing and purging times were no longer than in a typical ZnO ALD process, although a number of studies reported purging times as long as 30 s.

The characteristics of the interface between ZnO and Al_2O_3 in core–shell and nanolaminate structures have received some attention due to the Kirkendall effect that can be observed between the ZnO and Al_2O_3 phases at high temperatures (600–800 °C), causing the formation of voids and the spinel phase $ZnAl_2O_4$ [200, 217–219]. This effect can be exploited to improve the performance of the material in various applications; e.g. it has been shown to improve the luminescence properties of ZnO through reduction of the stress within ZnO grains [218]. In one study the effect was also utilized to obtain $ZnAl_2O_4$ by depositing a ZnO film on Al_2O_3 particles with ALD [220].

5.4. Hybrid thin films of ZnO

Inorganic–organic hybrid thin films deposited using a combination of ALD and MLD (molecular layer deposition) are a relatively new research topic within the ALD field, and ZnO has been used as the inorganic component in studies where the goal was either to deposit nanolaminates of ZnO and Zn hybrids [221, 222] or to fabricate hybrid superlattice structures of single organic layers between thicker ZnO layers [223, 224]. An illustration of a superlattice structure consisting of hydroquinone layers within the ZnO structure is shown in figure 3. These types of structures have a lot of potential in improving ZnO's performance in a number of applications through nanoscale confinement effects and the combination of inorganic and organic material properties.

6. Applications of ALD ZnO thin films

The attractive material property combination of ZnO, i.e. controllable conductivity, transparency to visible light, direct band gap of 3.37 eV and relatively high carrier mobility, combined with its low cost and ease of manufacture has led to its consideration for a wide variety of applications, including TFTs, UV LEDs, solar cells and gas sensors. ALD-grown ZnO has been used for all of these purposes, in many cases quite extensively as well. TCOs, another highly researched potential application for ZnO, will not be discussed here because the lowering of ZnO's resistivity through substitution, the typical approach for making TCOs, was already covered in section 3.

6.1. Thin film transistors

Zinc oxide can be used in TFTs as the active channel layer, which requires a low carrier concentration and high mobility for optimum performance. Because TFTs are primarily used in liquid-crystal displays, the components should also possess a high degree of transparency. The interest in using ALD for the fabrication of ZnO TFTs stems from the high quality and large-area uniformity of the resultant thin films as well as the relatively low deposition temperatures, which enables the use of organic dielectric components in the TFT.

Both thermal ALD [225–234] and PEALD [235–238] have been utilized in the fabrication of ZnO-based TFTs. While thermal ALD is the more commonly used technique for TFT fabrication, PEALD can offer the advantage of more reactive precursors, which can lead to fewer defects in the ZnO film and thus lower carrier concentration. Due to the carrier concentration and mobility requirements, the reported deposition temperatures are generally relatively low, typically in the 100–150 °C range. Controlling the deposition temperature remains the principal way of affecting the carrier concentration and mobility of the ZnO channel layer, although there are some studies where nitrogen doping was used to tune the electrical properties of ALD ZnO films [239–241].

6.2. Solar cell applications

ZnO's properties combined with the advantages of ALD have resulted in its use in multiple roles in thin-film solar cell research. The first applications considered for ZnO in the field were as buffer layers for Cu(InGa)Se_2 (CIGS) solar cells [242–247]. Here ZnO offered an alternative to the conventionally used CdS buffer layers, thus avoiding the use of the toxic cadmium. In addition to high optical transmittance, the buffer layers required high resistivity, so undoped ZnO was deposited at relatively low temperatures (120–160 °C) for this purpose. Later the focus of the use of ALD ZnO in solar cell applications has shifted to organic photovoltaics [248–255] and dye-sensitized solar cells (DSSCs) [256–258], where ZnO's chemical inertness, high conductivity and mobility as well as low work function have made it suitable for use as protective layers, electron-selective layers and photoanodes. Due to the thermal sensitivity of the organic parts of the cells, the reported deposition temperatures are generally quite low, typically under 100 °C. While the use of ZnO in organic solar cells only requires deposition on low-aspect-ratio surfaces, DSSCs, where ZnO has been used both as a photoanode and a blocking layer to reduce recombination, involve the coating of very high-aspect-ratio networks of nanoscale wires or fibers. Other uses for ZnO in solar cells include buffer layers for amorphous Si solar cells [259] and transparent conducting layers, which

have been used with CIGS cells [260] as well as Si thin-film solar cells [261].

6.3. Light-emitting diodes

ZnO's direct band gap of 3.37 eV and its large exciton binding energy of 60 meV make it a promising material for LED devices in the UV range. Due to the lack of reliable p-type doping of ZnO, its use in LEDs is limited to heterojunction devices, and the majority of reports on the use of ALD ZnO in LEDs use GaN as the p-type part of the junction [262–270]. Most of these studies utilize MOCVD for the fabrication of the GaN layers and ALD for ZnO. ALD is used mainly to ensure high quality of the ZnO layer, although some studies also employ ALD to fabricate a ZnO-coated SiO_2 nanoparticle layer between the junctions to act as a current blocking layer [262, 263, 266]. The light emission from these setups is mostly reported to be in the UV range [262–264, 266, 269], but some studies report white [265] or blue emission [267, 268, 270]. Another commonly studied LED junction is ALD ZnO together with Si or SiO_2-based materials [271–274], where the devices are designed either to enhance the photoluminescence properties of Si/SiO_2 [271] or to modify those of ZnO [272–274].

In addition to ZnO's applicability as the n-junction material in LEDs, Al-doped ZnO has also been used as a current spreading layer in InGaN/GaN LEDs [275] and as a buffer layer in organic LEDs [276], where the high conductivity of ZnO films facilitates control of the current in various layers of the LED and therefore improves performance. Another use for ZnO's optical properties that has been investigated using ALD are UV photodetectors, which utilize ZnO's band gap in a p–n junction or metal–semiconductor–metal configuration to detect UV radiation [277–279]. Core–shell nanowire structures can be used to improve the light capturing efficiency of such photodetectors, making ALD-grown ZnO thin films very promising for improving the performance of UV-range detectors.

6.4. Gas sensing and other applications

Gas sensing is a potential application for ZnO that has been gathering interest in the ALD field as well. The technology is based on chemiresistors, i.e. devices that exhibit a change in their resistivity upon the adsorption of molecules on their surface. Metal oxides can be used as the sensing part of the device because surface oxygen reacting with the gaseous species will induce a charge transfer between the surface and the bulk that will affect the resistivity of the material [191]. Core–shell ZnO nanofibers are fabricated for this purpose to maximize the surface-to-volume ratio and can be used in sensing gaseous molecules such as ethanol [163], CO [280], H_2 [281], NO_2, O_2 [196] and O_3 [282].

The applications described above are the most commonly researched applications for ALD-grown ZnO, but there are also a range of applications for ZnO that so far have not attracted quite the same level of attention within the field of ALD. Those applications include Schottky diodes [283, 284], non-volatile memory devices [285, 286], organic hybrid diodes [14, 287, 288], coatings for Li-ion battery electrodes [289, 290], gas-permeation barriers [291], radio frequency microelectromechanical systems [292] and paper deacidification [293], among others.

7. Conclusions and outlook

Compared to other thin-film deposition methods, the use of ALD was long held back by its relatively slow deposition rate, but as the technology has matured and the demands of many applications, particularly microelectronics, have increased, the advantages of ALD have made it an attractive choice for the deposition of thin films in demanding applications. With the ever decreasing scale of many novel applications, the high degree of conformality that can be achieved with ALD will further increase the importance of the technology in the coming years. The ALD process of ZnO has been thoroughly researched and the relevant process mechanisms already well understood, so the majority of ZnO ALD research from now on will concentrate on novel nanostructures and applications, as it has been for some years already. Novel material combinations such as the use of bio-templates and the fabrication of inorganic–organic hybrid structures have been demonstrated in recent years and will doubtless be explored further. Considering the wide variety of applications projected for ZnO and the versatility of the material, the trend of increasing interest in the ALD of ZnO shows no sign of abatement in the near future.

Acknowledgments

This work was supported by grants from Academy of Finland (no. 255562) and Aalto Energy Efficiency Research Programme.

References

[1] Coleman V A and Jagadish C 2006 *Zinc Oxide Bulk, Thin Films and Nanostructures* ed C Jagadish and S J Pearton (Amsterdam: Elsevier) pp 1–20
[2] Janotti A and Van de Walle C G 2009 *Rep. Prog. Phys.* **72** 126501
[3] Karpina V A *et al* 2004 *Cryst. Res. Technol.* **39** 980
[4] Kohan A F, Ceder G, Morgan D and Van de Walle C G 2000 *Phys. Rev.* B **61** 15019
[5] Van de Walle C G 2001 *Physica* B **308–310** 899
[6] Janotti A and Van de Walle C G 2006 *J. Cryst. Growth* **287** 58
[7] Kajikawa Y 2006 *J. Cryst. Growth* **289** 387
[8] Park W I 2008 *Met. Mater. Int.* **14** 659
[9] Willander M *et al* 2009 *Nanotechnology* **20** 332001
[10] Triboulet R and Perrière J 2003 *Prog. Cryst. Growth Charact. Mater.* **47** 65
[11] Ohtomo A and Tsukazaki A 2005 *Semicond. Sci. Technol.* **20** S1
[12] Lorenz M 2008 *Springer Ser. Mater. Sci.* **104** 303
[13] Chen M-J, Yang J-R and Shiojiri M 2012 *Semicond. Sci. Technol.* **27** 074005
[14] Luka G, Godlewski M, Guziewicz E, Stakhira P, Cherpak V and Volynyuk D 2012 *Semicond. Sci. Technol.* **27** 074006
[15] Tammenmaa M, Koskinen T, Hiltunen L and Niinistö L 1985 *Thin Solid Films* **124** 125

[16] Tanskanen J T, Bakke J R, Pakkanen T A and Bent S F 2011 *J. Vac. Sci. Technol.* A **29** 031507

[17] Kopalko K, Wójcik A, Godlewski M, Łusakowska E, Paszkowicz W, Domagała J Z, Godlewski M M, Szczerbakow A, Świątek K and Dybko K 2005 *Phys. Status Solidi* **2** 1125

[18] An K-S, Cho W, Lee B K, Lee S S and Kim C G 2008 *J. Nanosci. Nanotechnol.* **8** 4856

[19] Kobayashi K and Okudaira S 1997 *Chem. Lett.* **26** 511

[20] Wójcik A, Godlewski M, Guziewicz E, Minikayev R and Paszkowicz W 2008 *J. Cryst. Growth* **310** 284

[21] Guziewicz E *et al* 2009 *J. Appl. Phys.* **105** 122413

[22] Lujala V, Skarp J, Tammenmaa M and Suntola T 1994 *Appl. Surf. Sci.* **82/83** 34

[23] Sang B and Konagai M 1996 *Japan. J. Appl. Phys.* **35** L602

[24] Yamada A, Sang B and Konagai M 1997 *Appl. Surf. Sci.* **112** 216

[25] Saito K, Watanabe Y, Takahashi K, Matsuzawa T, Sang B and Konagai M 1997 *Sol. Energy Mater. Sol. Cells* **49** 187

[26] Ott A W and Chang R P H 1999 *Mater. Chem. Phys.* **58** 132

[27] Yousfi E B, Fouache J and Lincot D 2000 *Appl. Surf. Sci.* **153** 223

[28] Elam J W, Sechrist Z A and George S M 2002 *Thin Solid Films* **414** 43

[29] Park S-H K and Lee Y E 2004 *J. Mater. Sci.* **39** 2195

[30] Kim S K, Hwang C S, Park S-H K and Yun S J 2005 *Thin Solid Films* **478** 103

[31] Lee S, Im Y H, Kim S H and Hahn Y B 2006 *Superlattice Microstruct.* **39** 24

[32] Park S-H K, Hwang C-S, Kwack H-S, Lee J-H and Chu H Y 2006 *Electrochem. Solid State* **9** G299

[33] Lim J and Lee C 2007 *Thin Solid Films* **515** 3335

[34] Guziewicz E, Kowalik I A, Godlewski M, Kopalko K, Osinniy V, Wójcik A, Yatsunenko S, Łusakowska E, Paszkowicz W and Guziewicz M 2008 *J. Appl. Phys.* **103** 033515

[35] Jeon S, Bang S, Lee S, Kwon S, Jeong W, Jeon H, Chang H J and Park H-H 2008 *J. Electrochem. Soc.* **155** H738

[36] Lin P-Y, Gong J-R, Li P-C, Lin T-Y, Lyu D-Y, Lin D-Y, Lin H-J, Li T-C, Chang K-J and Lin W-J 2008 *J. Cryst. Growth* **310** 3024

[37] Makino H, Kishimoto S, Yamada T, Miyake A, Yamamoto N and Yamamoto T 2008 *Phys. Status Solidi* a **205** 1971

[38] Pung S-Y, Choy K-L, Hou X and Shan C 2008 *Nanotechnology* **19** 435609

[39] Kim C R *et al* 2008 *Solid State Commun.* **148** 395

[40] Makino H, Miyake A, Yamada T, Yamamoto N and Yamamoto T 2009 *Thin Solid Films* **517** 3138

[41] Krajewski T, Guziewicz E, Godlewski M, Wachnicki L, Kowalik I A, Wojcik-Glodowska A, Lukasiewicz M, Kopalko K, Osinniy V and Guziewicz M 2009 *Microelectron. J.* **40** 293

[42] Rowlette P C, Allen C G, Bromley O B, Dubetz A E and Wolden C A 2009 *Chem. Vapor Depos.* **15** 15

[43] Lin Y-T, Chung P-H, Lai H-W, Su H-L, Lyu D-Y, Yen K-Y, Lin T-Y, Kung C-Y and Gong J-R 2009 *Appl. Surf. Sci.* **256** 819

[44] Chung P-H, Lai H-W, Lin Y-T, Yen K-Y, Kung C-Y and Gong J-R 2009 *ECS Trans.* **19** 167

[45] Yen K-Y, Liu K-P, Lin Y-T, Gong J-R, Tsai K-Y, Lyu D-Y, Lin T-Y, Liang S-C, Ni G-Y and Jih F-W 2009 *ECS Trans.* **19** 843

[46] Kwon S-K, Kim D-W, Jung Y-H and Lee B-J 2009 *J. Korean Phys. Soc.* **55** 999

[47] Luka G, Krajewski T, Wachnicki L, Witkowski B, Lusakowska E, Paszkowicz W, Guziewicz E and Godlewski M 2010 *Phys. Status Solidi* a **207** 1568

[48] Guziewicz E *et al* 2010 *Phys. Status Solidi* b **247** 1611

[49] Gong S C, Bang S, Jeon H, Park H-H, Chang Y-C and Chang H J 2010 *Met. Mater. Int.* **16** 953

[50] Kim J-E, Bae S-M, Yang H and Hwang J-H 2010 *J. Korean Ceram. Soc.* **47** 353

[51] Min Y-S, An C J, Kim S K, Song J and Hwang C S 2010 *Bull. Korean Chem. Soc.* **31** 2503

[52] Kim D, Kang H, Kim J-M and Kim H 2011 *Appl. Surf. Sci.* **257** 3776

[53] Chiang T-Y, Dai C-L and Lian D-M 2011 *J. Alloys Compounds* **509** 5623

[54] Kawamura Y, Hattori N, Miyatake N, Horita M and Uraoka Y 2011 *Japan. J. Appl. Phys.* **50** 04DF05

[55] Kawamura Y, Hattori N, Miyatake N and Uraoka Y 2013 *J. Vac. Sci. Technol.* A **31** 01A142

[56] Cheng Y-C, Kuo Y-S, Li Y-H, Shyue J-J and Chen M-J 2011 *Thin Solid Films* **519** 5558

[57] Malm J, Sahramo E, Perälä J, Sajavaara T and Karppinen M 2011 *Thin Solid Films* **519** 5319

[58] Kudrawiec R, Misiewicz J, Wachnicki Ł, Guziewicz E and Godlewski M 2011 *Semicond. Sci. Technol.* **26** 075012

[59] Janocha E and Pettenkofer C 2011 *Appl. Surf. Sci.* **257** 10031

[60] Tapily K, Gu D, Baumgart H, Namkoong G, Stegall D and Elmustafa A A 2011 *Semicond. Sci. Technol.* **26** 115005

[61] Lin M-C, Wu M-K, Yuan K-Y, Chen M-J, Yang J-R and Shiojiri M 2011 *J. Electrochem. Soc.* **158** H1213

[62] Nam T, Kim J-M, Kim M-K, Kim H and Kim W-H 2011 *J. Korean Phys. Soc.* **59** 452

[63] Pradhan K and Lyman P F 2011 *ECS Trans.* **41** 247

[64] Wang T, Wu H, Chen C and Liu C 2012 *Appl. Phys. Lett.* **100** 011901

[65] Illiberi A, Roozeboom F and Poodt P 2012 *ACS Appl. Mater. Interfaces* **4** 268

[66] Mousa M B M, Oldham C J, Jur J S and Parsons G N 2012 *J. Vac. Sci. Technol.* A **30** 01A155

[67] Thomas M A and Cui J B 2012 *ACS Appl. Mater. Interfaces* **4** 3122

[68] Zhimin C, Xinchun L and Dannong H 2012 *Surf. Coat. Technol.* **207** 361

[69] Baji Z, Lábadi Z, Horváth Z E, Molnár G, Volk J, Bársony I and Barna P 2012 *Cryst. Growth Des.* **12** 5615

[70] Sultan S M, Clark O D, Masaud T B, Fang Q, Gunn R, Hakim M M A, Sun K, Ashburn P and Chong H M H 2012 *Microelectron. Eng.* **97** 162

[71] Huang H-W, Chang W-C, Lin S-J and Chueh Y-L 2012 *J. Appl. Phys.* **112** 124102

[72] Yuan N Y, Wang S Y, Tan C B, Wang X Q, Chen G G and Ding J N 2013 *J. Cryst. Growth* **366** 43

[73] Čeh M, Chen H-C, Chen M-J, Yang J-R and Shiojiri M 2010 *Mater. Trans.* **51** 219

[74] Dasgupta N P, Neubert S, Lee W, Trejo O, Lee J-R and Prinz F B 2010 *Chem. Mater.* **22** 4769

[75] Lee D-J, Kim H-M, Kwon J-Y, Choi H, Kim S-H and Kim K-B 2011 *Adv. Funct. Mater.* **21** 448

[76] Lee D-J, Kwon J-Y, Kim S-H, Kim H-M and Kim K-B 2011 *J. Electrochem. Soc.* **158** D277

[77] Geng Y, Xie Z-Y, Xu S-S, Sun Q-Q, Ding S-J, Lu H-L and Zhang D W 2012 *ECS J. Solid State Sci. Technol.* **1** N45

[78] Baji Z, Lábadi Z, Horváth Z E and Bársony I 2012 *Thin Solid Films* **520** 4703

[79] Yuan H, Luo B, Yu D, Cheng A-J, Campbell S A and Gladfelter W L 2012 *J. Vac. Sci. Technol.* A **30** 01A138

[80] Genevée P, Donsanti F, Renou G and Lincot D 2013 *Appl. Surf. Sci.* **264** 464

[81] Frölich A and Wegener M 2011 *Opt. Mater. Express* **1** 883

[82] Luka G, Wachnicki L, Witkowski B S, Krajewski T A, Jakiela R, Guziewicz E and Godlewski M 2011 *Mater. Sci. Eng.* B **176** 237
[83] Luka G, Krajewski T A, Witkowski B S, Wisz G, Virt I S, Guziewicz E and Godlewski M 2011 *J. Mater. Sci., Mater. Electron.* **22** 1810
[84] Cheng Y-C 2011 *Appl. Surf. Sci.* **258** 604
[85] Dhakal T, Vanhart D, Christian R, Nandur A, Sharma A and Westgate C R 2012 *J. Vac. Sci. Technol.* A **30** 021202
[86] Banerjee P, Lee W-J, Bae K-R, Lee S B and Rubloff G W 2010 *J. Appl. Phys.* **108** 043504
[87] Kwon S J 2005 *Japan. J. Appl. Phys.* **44** 1062
[88] Maeng W J, Lee J-W, Lee J H, Chung K-B and Park J-S 2011 *J. Phys. D: Appl. Phys.* **44** 445305
[89] Maeng W J, Kim S-J, Park J-S, Chung K-B and Kim H 2012 *J. Vac. Sci. Technol.* B **30** 031210
[90] Hou Q, Meng F and Sun J 2013 *Nanoscale Res. Lett.* **8** 144
[91] Mundle R M, Terry H S, Santiago K, Shaw D, Bahoura M, Pradhan A K, Dasari K and Palai R 2013 *J. Vac. Sci. Technol.* A **31** 01A146
[92] Tynell T, Okazaki R, Terasaki I, Yamauchi H and Karppinen M 2013 *J. Mater. Sci.* **48** 2806
[93] Tynell T, Okazaki R, Terasaki I, Yamauchi H and Karppinen M 2013 *J. Vac. Sci. Technol.* A **31** 01A109
[94] Ahn C H, Kim H and Cho H K 2010 *Thin Solid Films* **519** 747
[95] Elam J W and George S M 2003 *Chem. Mater.* **15** 1020
[96] Elam J W, Routkevitch D and George S M 2003 *J. Electrochem. Soc.* **150** G339
[97] Na J-S, Peng Q, Scarel G and Parsons G N 2009 *Chem. Mater.* **21** 5585
[98] Na J-S, Scarel G and Parsons G N 2010 *J. Phys. Chem.* C **114** 383
[99] Yamamoto Y, Saito K, Takahashi K and Konagai M 2001 *Sol. Energy Mater. Sol. Cells* **65** 125
[100] Sang B, Yamada A and Konagai M 1997 *Sol. Energy Mater. Sol. Cells* **49** 19
[101] Sang B, Yamada A and Konagai M 1998 *Japan. J. Appl. Phys.* **37** L206
[102] Chalker P R, Marshall P A, Romani S, Roberts J W, Irvine S J C, Lamb D A, Clayton A J and Williams P A 2013 *J. Vac. Sci. Technol.* A **31** 01A120
[103] Saito K, Hiratsuka Y, Omata A, Makino H, Kishimoto S, Yamamoto T, Horiuchi N and Hirayama H 2007 *Superlattices Microstruct.* **42** 172
[104] Chalker P R, Marshall P A, King P J, Dawson K, Romani S, Williams P A, Ridealgh J and Rosseinsky M J 2012 *J. Mater. Chem.* **22** 12824
[105] Thomas M A, Armstrong J C and Cui J 2013 *J. Vac. Sci. Technol.* A **31** 01A130
[106] Ahn C H, Kim J H and Cho H K 2012 *J. Electrochem. Soc.* **159** H384
[107] Lee C and Lim J 2006 *J. Vac. Sci. Technol.* A **24** 1031
[108] Lee C, Park S Y, Lim J and Kim H W 2007 *Mater. Lett.* **61** 2495
[109] Dunlop L, Kursumovic A and MacManus-Driscoll J L 2008 *Appl. Phys. Lett.* **93** 172111
[110] Kim H S, Lee D H and Noh S J 2011 *J. Korean Phys. Soc.* **58** 761
[111] Yuan H, Luo B, Campbell S A and Gladfelter W L 2011 *Electrochem. Solid-State Lett.* **14** H181
[112] Shih Y T, Chien J F, Chen M J, Yang J R and Shiojiri M 2011 *J. Electrochem. Soc.* **158** H516
[113] Park H H, Heasley R and Gordon R G 2013 *Appl. Phys. Lett.* **102** 132110
[114] Jeon S, Bang S, Lee S, Kwon S, Jeong W, Jeon H, Chang H J and Park H-H 2008 *J. Korean Phys. Soc.* **53** 3287
[115] Bakke J R, Tanskanen J T, Hägglund C, Pakkanen T A and Bent S F 2012 *J. Vac. Sci. Technol.* A **30** 01A135
[116] Yuan H 2012 *J. Mater. Sci. Mater. Electron.* **23** 2075
[117] Kapilashrami M, Kronawitter C X, Törndahl T, Lindahl J, Hultqvist A, Wang W-C, Chang C-L, Mao S S and Guo J 2012 *Phys. Chem. Chem. Phys.* **14** 10154
[118] Ye Z-Y, Lu H-L, Geng Y, Gu Y-Z, Xie Z-Y, Zhang Y, Sun Q-Q, Ding S-J and Zhang D W 2013 *Nanoscale Res. Lett.* **8** 108
[119] Lin M-C, Chang Y-J, Chen M-J and Chu C-J 2011 *J. Electrochem Soc.* **158** D395
[120] Kaiya K, Yoshii N, Takahashi N and Nakamura T 2000 *J. Mater. Sci. Lett.* **19** 2089
[121] Kopalko K, Godlewski M, Domagala J Z, Lusakowska E, Minikayev R, Paszkowicz W and Szczerbakow A 2004 *Chem. Mater.* **16** 1447
[122] Kopalko K, Godlewski M, Łusakowska E, Paszkowicz W, Domagała J Z, Szczerbakow A, Ivanov V Y, Godlewski M M and Phillips M R 2004 *Phys. Status Solidi* c **1** 892
[123] Liu C H, Yan M, Liu X, Seelig E and Chang R P H 2002 *Chem. Phys. Lett.* **355** 43
[124] Saito K, Nagayama K, Hosokai Y, Ishida K and Takahashi K 2004 *Phys. Status Solidi* c **1** 969
[125] Shin K and Lee C 2004 *Phys. Status Solidi* c **1** 2545
[126] Lim J, Shin K, Kim H W and Lee C 2004 *J. Lumin.* **109** 181
[127] Lim J, Shin K, Kim H and Lee C 2005 *Thin Solid Films* **475** 256
[128] Lee C, Park S Y and Lim J 2007 *J. Korean Phys. Soc.* **50** 590
[129] Murata M, Tanaka Y, Sanjo Y, Kumagai H, Shinagawa T and Chigane M 2011 *Proc. SPIE* **7927** 79270Q
[130] Kumagai H, Tanaka Y, Murata M, Masuda Y and Shinagawa T 2010 *J. Phys.: Condens. Matter* **22** 474008
[131] Yang S, Lin B H, Liu W-R, Lin J-H, Chang C-S, Hsu C-H and Hsieh W F 2009 *Cryst. Growth Des.* **9** 5184
[132] Ku C-S, Huang J-M, Lin C-M and Lee H-Y 2009 *Thin Solid Films* **518** 1373
[133] Ku C-S, Lee H-Y, Huang J-M and Lin C-M 2010 *Mater. Chem. Phys.* **120** 236
[134] Ku C-S, Lee H-Y, Huang J-M and Lin C-M 2010 *Cryst. Growth Des.* **10** 1460
[135] Wachnicki Ł, Krajewski T, Łuka G, Witkowski B, Kowalski B, Kopalko K, Domagala J Z, Guziewicz M, Godlewski M and Guziewicz E 2010 *Thin Solid Films* **518** 4556
[136] Wachnicki Ł *et al* 2010 *Phys. Status Solidi* b **247** 1699
[137] Chen H C, Chen M J, Liu T C, Yang J R and Shiojiri M 2010 *Thin Solid Films* **519** 536
[138] Knez M, Nielsch K and Niinistö L 2007 *Adv. Mater.* **19** 3425
[139] Subannajui K, Güder F, Danhof J, Menzel A, Yang Y, Kirste L, Wang C, Cimalla V, Schwarz U and Zacharias M 2012 *Nanotechnology* **23** 235607
[140] Ra H-W, Choi K-S, Kim J-H, Hahn Y-B and Im Y-H 2008 *Small* **4** 1105
[141] Sultan S M, Sun K, Clark O D, Masaud T B, Fang Q, Gunn R, Partridge J, Allen M W, Ashburn P and Chong H M H 2012 *IEEE Electron Device Lett.* **33** 203
[142] Chang Y-H, Wang S-M, Liu C-M and Chen C 2010 *J. Electrochem. Soc.* **157** K236
[143] Lim Y T, Son J Y and Rhee J-S 2013 *Ceram. Int.* **39** 887
[144] Norek M, Łuka G, Godlewski M, Płociński T, Michalska-Domańska M and Stępniowski W J 2013 *Appl. Phys.* A **111** 265
[145] Güder F, Yang Y, Krüger M, Stevens G B and Zacharias M 2010 *ACS Appl. Mater. Interfaces* **2** 3473
[146] Subannajui K, Menzel A, Güder F, Yang Y, Schumann K, Lu X and Zacharias M 2013 *Adv. Funct. Mater.* **23** 191
[147] Wu M K, Shih Y T, Chen M J, Yang J R and Shiojiri M 2009 *Phys. Status Solidi RRL* **3** 88

[148] Pourret A, Guyot-Sionnest P and Elam J W 2009 *Adv. Mater.* **21** 232
[149] Kim H W, Shim S H and Lee J W 2007 *Thin Solid Films* **515** 6433
[150] Zhu Z *et al* 1997 *Phys. Status Solidi* b **202** 827
[151] Wu M-K, Chen M-J, Tsai F-Y, Yang J-R and Shiojiri M 2010 *Mater. Trans.* **51** 253
[152] Qian K-J, Chen S, Zhu B, Chen L, Ding S-J, Lu H-L, Sun Q-Q, Zhang D W and Chen Z 2012 *Appl. Surf. Sci.* **258** 4657
[153] Li Q, Kumar V, Li Y, Zhang H, Marks T J and Chang R P H 2005 *Chem. Mater.* **17** 1001
[154] Solis-Pomar F, Martinez E, Meléndrez M F and Pérez-Tijerina E 2011 *Nanoscale Res. Lett.* **6** 524
[155] Meléndrez M F, Hanks K, Leonard-Deepak F, Solis-Pomar F, Martinez-Guerra E, Pérez-Tijerina E and José-Yacaman M 2012 *J. Mater. Sci.* **47** 2025
[156] Ding J N, Liu Y B, Tan C B and Yuan N Y 2012 *Nanoscale Res. Lett.* **7** 368
[157] Baek S-H, Noh B-Y, Park I-K and Kim J H 2012 *Nanoscale Res. Lett.* **7** 29
[158] Cao C-W, Bao W-N, Lin X, Liu X-Y, Geng Y, Lu H-L, Sun Q-Q, Zhou P, Zhang D W and Wang P-F 2013 *ECS Solid State Lett.* **2** Q25
[159] Elam J W, Routkevitch D, Mardilovich P P and George S M 2003 *Chem. Mater.* **15** 3507
[160] Bae C, Zierold R, Montero Moreno J M, Kim H, Shin H, Bachmann J and Nielsch K 2013 *J. Mater. Chem.* C **1** 621
[161] Lee H-Y, An C J, Piao S J, Ahn D Y, Kim M-T and Min Y-S 2010 *J. Phys. Chem.* C **114** 18601
[162] Park J Y, Choi S-W and Kim S S 2010 *Nanotechnology* **21** 475601
[163] Cho S, Kim D-H, Lee B-S, Jung J, Yu W-R, Hong S-H and Lee S 2012 *Sensors Actuators* B **162** 300
[164] Fang X, Li S, Wang X, Fang F, Chu X, Wei Z, Li J, Chen X and Wang F 2012 *Appl. Surf. Sci.* **263** 14
[165] Kayaci F, Ozgit-Akgun C, Donmez I, Biyikli N and Uyar T 2012 *ACS Appl. Mater. Interfaces* **4** 6185
[166] Kayaci F, Ozgit-Akgun C, Biyikli N and Uyar T 2013 *RSC Adv.* **3** 6817
[167] Suresh V, Huang M S, Srinivasan M P, Guan C, Fan H J and Krishnamoorthy S 2012 *J. Phys. Chem.* C **116** 23729
[168] Oldham C J, Gong B, Spagnola J C, Jur J S, Senecal K J, Godfrey T A and Parsons G N 2010 *ECS Trans.* **33** 279
[169] Gong B, Peng Q, Na J-S and Parsons G N 2011 *Appl. Catal.* A **407** 211
[170] Ras R H A, Sahramo E, Malm J, Raula J and Karppinen M 2008 *J. Am. Chem. Soc.* **130** 11252
[171] Malm J, Sahramo E, Karppinen M and Ras R H A 2010 *Chem. Mater.* **22** 3349
[172] Lee S-M, Grass G, Kim G-M, Dresbach C, Zhang L, Gösele U and Knez M 2009 *Phys. Chem. Chem. Phys.* **11** 3608
[173] Korhonen J T, Hiekkataipale P, Malm J, Karppinen M, Ikkala O and Ras R H A 2011 *ACS Nano* **5** 1967
[174] Chang Y-M, Kao P-H, Liu M-C, Lin C-M, Lee H-Y and Juang J-Y 2012 *RSC Adv.* **2** 11089
[175] Libera J A, Elam J W and Pellin M J 2008 *Thin Solid Films* **516** 6158
[176] King D M, Liang X, Carney C S, Hakim L F, Li P and Weimer A W 2008 *Adv. Funct. Mater.* **18** 607
[177] King D M, Johnson S I, Li J, Du X, Liang X and Weimer A W 2009 *Nanotechnology* **20** 195401
[178] King D M, Li J, Liang X, Johnson S I, Channel M M and Weimer A W 2009 *Cryst. Growth Des.* **9** 2828
[179] King D M, Liang X, Li P and Weimer A W 2008 *Thin Solid Films* **516** 8517
[180] Rauwel E, Nilsen O, Galeckas A, Walmsley J C, Rytter E and Fjellvåg H 2011 *ECS Trans.* **41** 123
[181] Alessandri I, Zucca M, Ferroni M, Bontempi E and Depero L E 2009 *Cryst. Growth Des.* **9** 1258
[182] Ferguson J D, Weimer A W and George S M 2005 *J. Vac. Sci. Technol.* A **23** 118
[183] Clavel G, Marichy C, Willinger M-G, Ravaine S, Zitoun D and Pinna N 2010 *Langmuir* **26** 18400
[184] Zhang Z, Patterson M, Ren M, Wang Y, Flake J C, Sprunger P T and Kurtz R L 2013 *J. Vac. Sci. Technol.* A **31** 01A144
[185] Kim H W, Shim S H and Lee J W 2008 *Nanotechnology* **19** 145601
[186] Kong B H, Choi M K, Cho H K, Kim J H, Baek S and Lee J-H 2010 *Electrochem. Solid-State Lett.* **13** K12
[187] Chang Y-M, Jian S-R, Lee H-Y, Lin C-M and Juang J-Y 2010 *Nanotechnology* **21** 385705
[188] Chang Y-M, Shieh J, Chu P-Y, Lee H-Y, Lin C-M and Juang J-Y 2011 *ACS Appl. Mater. Interfaces* **3** 4415
[189] Chang Y-M, Liu M-C, Kao P-H, Lin C-M, Lee H-Y and Juang J-Y 2012 *ACS Appl. Mater. Interfaces* **4** 1411
[190] Kale V S, Ramanujam Prabhakar R, Pramana S S, Rao M, Sow C-H, Jinesh K B and Mhaisalkar S G 2012 *Phys. Chem. Chem. Phys.* **14** 4614
[191] Dobrokhotov V *et al* 2012 *J. Appl. Phys.* **111** 044311
[192] Dobrokhotov V *et al* 2012 *Sensors Actuators* B **168** 138
[193] Li H-H, Yang C-E, Kei C-C, Su C-Y, Dai W-S, Tseng J-K, Yang P-Y, Chou J-C and Cheng H-C 2013 *Thin Solid Films* **529** 173
[194] Han H-C *et al* 2013 *Nano Lett.* **13** 1422
[195] Park S, Kim H, Lee J W, Kim H W and Lee C 2008 *J. Korean Phys. Soc.* **53** 657
[196] Choi S-W, Park J Y and Kim S S 2009 *Nanotechnology* **20** 465603
[197] Jin C, Kim H, Ryu H-Y, Kim H W and Lee C 2011 *J. Phys. Chem.* C **115** 8513
[198] Kim H, Jin C, Park S and Lee C 2012 *Mater. Res. Bull.* **47** 2708
[199] Park S, An S, Ko H, Jin C and Lee C 2013 *Ceram. Int.* **39** 3539
[200] Peng Q, Sun X-Y, Spagnola J C, Saquing C, Khan S A, Spontak R J and Parsons G N 2009 *ACS Nano* **3** 546
[201] Sun W-C, Yeh Y-C, Ko C-T, He J-H and Chen M-J 2011 *Nanoscale Res. Lett.* **6** 556
[202] Wang H-B, Ma F, Li Q-Q, Dong C-Z, Ma D-Y, Wang H-T and Xu K-W 2013 *Nanoscale* **5** 2857
[203] Li X L, Li C, Zhang Y, Chu D P, Milne W I and Fan H J 2010 *Nanoscale Res. Lett.* **5** 1836
[204] Lin Y-H, Lee P-S, Hsueh Y-C, Pan K-Y, Kei C-C, Chan M-H, Wu J-M, Perng T-P and Shih H C 2011 *J. Electrochem. Soc.* **158** K24
[205] Min Y-S, Lee I H, Lee Y H and Hwang C S 2011 *Cryst. Eng. Commun.* **13** 3451
[206] Park J Y, Choi S-W, Lee J-W, Lee C and Kim S S 2009 *J. Am. Ceram. Soc.* **92** 2551
[207] Park S, Jun J, Kim H W and Lee C 2009 *Solid State Commun.* **149** 315
[208] Janik E, Wachnicka A, Guziewicz E, Godlewski M, Kret S, Zaleszczyk W, Dynowska E, Presz A, Karczewski G and Wojtowicz T 2010 *Nanotechnology* **21** 015302
[209] Gas K *et al* 2011 *Phys. Status Solidi* b **248** 1592
[210] Kim H W, Yang J C, Na H G and Lee C 2011 *Appl. Surf. Sci.* **257** 9420
[211] Jin C, Kim H and Lee C 2011 *Cryst. Res. Technol.* **46** 1065
[212] Jin C, Park S, Kim H and Lee C 2012 *Sensors Actuators* B **161** 223
[213] Jin C, Kim H, Park S, Choi S-W, Kim S S and Lee C 2012 *Surf. Interface Anal.* **44** 1534
[214] Kim H, Jin C, Park S, Kwon Y, Lee S and Lee C 2012 *Phys. Scr.* **T149** 014052

[215] Bang S, Lee S, Park T, Ko Y, Shin S, Yim S-Y, Seo H and Jeon H 2012 *J. Mater. Chem.* **22** 14141
[216] An S, Park S, Ko H and Lee C 2012 *Appl. Phys.* A **108** 53
[217] Jang Y W, Bang S, Jeon H and Lee J Y 2011 *Phys. Status Solidi* b **248** 1634
[218] Güder F, Yang Y, Danhof J, Hartel A, Schwarz U T and Zacharias M 2011 *Appl. Phys. Lett.* **99** 023105
[219] Güder F, Yang Y, Goetze S, Berger A, Scholz R, Hiller D, Hesse D and Zacharias M 2011 *Chem. Mater.* **23** 4445
[220] Rauwel E, Galeckas A, Rauwel P, Nilsen O, Walmsley J C, Rytter E and Fjellvåg H 2012 *J. Electrochem. Soc.* **159** P45
[221] Yoon B, Lee B H and George S M 2011 *ECS Trans.* **41** 271
[222] Yoon B, Lee B H and George S M 2012 *J. Phys. Chem.* C **116** 24784
[223] Tynell T and Karppinen M 2014 *Thin Solid Films* **551** 23
[224] Tynell T, Terasaki I, Yamauchi H and Karppinen M 2013 *J. Mater. Chem.* A **1** 13619
[225] Kwon S, Bang S, Lee S, Jeon S, Jeong W, Kim H, Gong S C, Chang H J, Park H-H and Jeon H 2009 *Semicond. Sci. Technol.* **24** 035015
[226] Bang S, Lee S, Jeon S, Kwon S, Jeong W, Kim H, Shin I, Chang H J, Park H-H and Jeon H 2009 *Semicond. Sci. Technol.* **24** 025008
[227] Choi W-S 2009 *J. Korean Phys. Soc.* **54** 678
[228] Moon Y-K, Lee S, Park J-W, Kim D-H, Lee J-H and Jeong C-O 2009 *J. Korean Phys. Soc.* **55** 1906
[229] Bang S, Lee S, Park J, Park S, Jeong W and Jeon H 2009 *J. Phys. D: Appl. Phys.* **42** 235102
[230] Kawamura Y, Horita M and Uraoka Y 2010 *Japan. J. Appl. Phys.* **49** 04DF19
[231] Zhao D, Mourey D A and Jackson T N 2010 *IEEE Electron Device Lett.* **31** 323
[232] Lee S, Bang S, Park J, Park S, Jeong W and Jeon H 2010 *Phys. Status Solidi* a **207** 1845
[233] Choi K M, Hyung G W, Yang J W, Koo J R, Kim Y K, Kwon S J and Cho E S 2010 *Mol. Cryst. Liq. Cryst.* **529** 131
[234] Yang J, Park J K, Kim S, Choi W, Lee S and Kim H 2012 *Phys. Status Solidi* a **209** 2087
[235] Mourey D A, Zhao D A, Sun J and Jackson T N 2010 *IEEE Trans. Electron Devices* **57** 530
[236] Lim S J, Kim J-M, Kim D, Lee C, Park J-S and Kim H 2010 *Electrochem. Solid-State Lett.* **13** H151
[237] Zhu C, Smith D J and Nemanich R J 2012 *J. Vac. Sci. Technol.* B **30** 051807
[238] Kawamura Y, Tani M, Hattori N, Miyatake N, Horita M, Ishikawa Y and Uraoka Y 2012 *Japan. J. Appl. Phys.* **51** 02BF04
[239] Lim S J, Kwon S-J, Kim H and Park J-S 2007 *Appl. Phys. Lett.* **91** 183517
[240] Kim J-M, Nam T, Lim S J, Seol Y G, Lee N-E, Kim D and Kim H 2011 *Appl. Phys. Lett.* **98** 142113
[241] Kim J-M, Lim S J, Nam T, Kim D and Kim H 2011 *J. Electrochem. Soc.* **158** J150
[242] Chaisitsak S, Sugiyama T, Yamada A and Konagai M 1999 *Japan. J. Appl. Phys.* **38** 4989
[243] Canava B, Guillemoles J-F, Yousfi E-B, Cowache P, Kerber H, Loeffl A, Schock H-W, Powalla M, Hariskos D and Lincot D 2000 *Thin Solid Films* **361–362** 187
[244] Chaisitsak S, Yamada A, Konagai M and Saito K 2000 *Japan. J. Appl. Phys.* **39** 1660
[245] Shimizu A, Chaisitsak S, Sugiyama T, Yamada A and Konagai M 2000 *Thin Solid Films* **361–362** 193
[246] Malm U, Malmström J, Platzer-Björkman C and Stolt L 2005 *Thin Solid Films* **480–481** 208
[247] Platzer-Björkman C, Törndahl T, Abou-Ras D, Malmström J, Kessler J and Stolt L 2006 *J. Appl. Phys.* **100** 044506
[248] Wang J-C, Weng W-T, Tsai M-Y, Lee M-K, Horng S-F, Perng T-P, Kei C-C, Yu C-C and Meng H-F 2010 *J. Mater. Chem.* **20** 862
[249] Stakhira P I, Pakhomov G L, Cherpak V V, Volynyuk D, Luka G, Godlewski M, Guziewicz E and Hotra Z Y 2010 *Cent. Eur. J. Phys.* **8** 798
[250] Stakhira P Y, Grygorchak I I, Cherpak V V, Ivastchyshyn F O, Volynyuk D Y, Luka G, Godlewski M, Guziewicz E, Pakhomov G L and Hotra Z Y 2010 *Mater. Sci. Eng.* B **172** 272
[251] Cheun H, Fuentes-Hernandez C, Zhou Y, Potscavage W J Jr, Kim S-J, Shim J, Dindar A and Kippelen B 2010 *J. Phys. Chem.* C **114** 20713
[252] Cheun H *et al* 2012 *Adv. Funct. Mater.* **22** 1531
[253] Park S-Y, Seo H O, Kim K-D, Lee J E, Kwon J-D, Kim Y D and Lim D C 2012 *Phys. Status Solidi RRL* **6** 196
[254] Lim D C *et al* 2012 *Energy Environ. Sci.* **5** 9803
[255] Kang Y-J, Kim C S, Kwack W-S, Ryu S Y, Song M, Kim D-H, Hong S W, Jo S, Kwon S-H and Kang J-W 2012 *ECS Solid State Lett.* **1** Q1
[256] Tétreault N, Heiniger L-P, Stefik M, Labouchère P P, Arsenault É, Nazeeruddin N K, Ozin G A and Grätzel M 2011 *ECS Trans.* **41** 303
[257] Williams V O, Jeong N C, Prasittichai C, Farha O K, Pellin M J and Hupp J T 2012 *ACS Nano* **6** 6185
[258] Ding J, Li Y, Hu H, Bai L, Zhang S and Yuan N 2013 *Nanoscale Res. Lett.* **8** 9
[259] Lee Y-J *et al* 2012 *J. Phys. Chem.* C **116** 23231
[260] Yousfi E B, Weinberger B, Donsanti F, Cowache P and Lincot D 2001 *Thin Solid Films* **387** 29
[261] Steglich M, Bingel A, Jia G and Falk F 2012 *Sol. Energy Mater. Sol. Cells* **103** 62
[262] Wu M K, Shih Y T, Li W C, Chen H C, Chen M J, Kuan H, Yang J R and Shiojiri M 2008 *IEEE Photonics Technol. Lett.* **20** 1772
[263] Shih Y T, Wu M K, Li W C, Kuan H, Yang J R, Shiojiri M and Chen M J 2009 *Nanotechnology* **20** 165201
[264] Chen H-C, Chen M-J, Wu M-K, Li W-C, Tsai H-L, Yang J-R, Kuan H and Shiojiri M 2010 *IEEE J. Quantum Electron.* **46** 265
[265] Chen H C, Chen M J, Huang Y H, Sun W C, Li W C, Yang J R, Kuan H and Shiojiri M 2011 *IEEE Trans. Electron Devices* **58** 3970
[266] Chen M-J, Yang J-R and Shiojiri M 2012 *Semicond. Sci. Technol.* **27** 074005
[267] Wang T, Wu H, Wang Z, Chen C and Liu C 2012 *Appl. Phys. Lett.* **101** 161905
[268] Wang T, Wu H, Wang Z, Chen C and Liu C 2013 *Nanoscale Res. Lett.* **8** 99
[269] Chien J-F, Liao H-Y, Yu S-F, Lin R-M, Shiojiri M, Shyue J-J and Chen M-J 2013 *ACS Appl. Mater. Interfaces* **5** 227
[270] Wang T, Wu H, Zheng H, Wang J B, Wang Z, Chen C, Xu Y and Liu C 2013 *Appl. Phys. Lett.* **102** 141912
[271] Sun E, Su F-H, Shih Y-T, Tsai H-L, Chen C-H, Wu M-K, Yang J-R and Chen M-J 2009 *Nanotechnology* **20** 445202
[272] Shih Y T, Wu M K, Chen M J, Cheng Y C, Yang J R and Shiojiri M 2010 *Appl. Phys.* B **98** 767
[273] Ku C-S, Huang J-M, Cheng C-Y, Lin C-M and Lee H-Y 2010 *Appl. Phys. Lett.* **97** 181915
[274] Lin M C, Wu M-K, Chen M-J, Yang J-R and Shiojiri M 2012 *Mater. Chem. Phys.* **135** 88
[275] Kong B H, Cho H K, Kim M Y, Choi R J and Kim B K 2011 *J. Cryst. Growth* **326** 147
[276] Choi Y-J, Gong S C, Park C-S, Lee H-S, Jang J G, Chang H J, Yeom G Y and Park H-H 2013 *ACS Appl. Mater. Interfaces* **5** 3650
[277] Shan C X, Zhang J Y, Yao B, Shen D Z, Fan X W and Choy K L 2009 *J. Vac. Sci. Technol.* B **27** 1765

[278] Kim D C, Jung B O, Kwon Y H and Cho H K 2012 *J. Electrochem. Soc.* **159** K10
[279] Kang H, Park J, Choi T, Jung H, Lee K H, Im S and Kim H 2012 *Appl. Phys. Lett.* **100** 041117
[280] Park J Y, Choi S-W and Kim S S 2011 *J. Phys. D: Appl. Phys.* **44** 205403
[281] Singh U, Lee H A, Byun Y-C, Kumar A, Seal S, Kim H and Cho H J 2011 *Procedia Eng.* **25** 1669
[282] Güder F *et al* 2012 *Small* **8** 3307
[283] Krajewski T A *et al* 2011 *Appl. Phys. Lett.* **98** 263502
[284] Ryu B, Lee Y T, Lee K H, Ha R, Park J H, Choi H-J and Im S 2011 *Nano Lett.* **11** 4246
[285] Huby N, Tallarida G, Kutrzeba M, Ferrari S, Guziewicz E, Wachnicki Ł and Godlewski M 2008 *Microelectron. Eng.* **85** 2442
[286] Oru F B, Cimen F, Rizk A, Ghaffari M, Nayfeh A and Okyay A K 2012 *IEEE Electron Device Lett.* **33** 1714
[287] Katsia E *et al* 2009 *Appl. Phys. Lett.* **94** 143501
[288] Lee K H, Park A, Im S, Park Y, Kim S H, Sung M M and Lee S 2010 *Electrochem. Solid-State Lett.* **13** H261
[289] Zhao J and Wang Y 2012 *J. Phys. Chem.* C **116** 11867
[290] Zhao J and Wang Y 2013 *J. Solid State Electrochem.* **17** 1049
[291] Chou C-T, Yu P-W, Tseng M-H, Hsu C-C, Shyue J-J, Wang C-C and Tsai F-Y 2013 *Adv. Mater.* **25** 1750
[292] Herrmann C F, DelRio F W, Miller D C, George S M, Bright V M, Ebel J L, Strawser R E, Cortez R and Leedy K D 2007 *Sensors Actuators* A **135** 262
[293] Hanson C A, Oldham C J and Parsons G N 2012 *J. Vac. Sci. Technol.* A **30** 01A117